Global analysis of specificity determinants in eukaryotic protein kinases

David Bradley[1], Cristina Viéitez[2], Vinothini Rajeeve[3], Pedro R. Cutillas[3], Pedro Beltrao[1*]

[1]European Molecular Biology Laboratory, European Bioinformatics Institute (EMBL-EBI), Wellcome Genome Campus, Cambridge CB10 1SD, UK
[2]European Molecular Biology Laboratory (EMBL), Genome Biology Unit, 69117 Heidelberg, Germany
[3]Integrative Cell Signalling & Proteomics, Centre for Haemato-Oncology, Barts Cancer Institute, Queen Mary University of London, Charterhouse Square, London, EC1M 6BQ

*Correspondence to: pbeltrao@ebi.ac.uk

Abstract

Protein kinases are at the heart of cell signalling processes, constitute one of the largest human domain families and are often mutated in disease. Kinase target recognition at the active-site is in part determined by a few amino-acids around the phosphoacceptor residue. These substrate preferences vary across kinases and despite the increased knowledge of target phosphosites little is known about how most preferences are encoded in the kinase sequence. Here, we used alignment-based approaches to identify 30 putative target sequence determinant residues (SDRs) for 16 substrate preferences that were further studied using structural models and 2 validated through activity assays of mutant kinases. Mutation data from patient cancer samples revealed that SDRs are often targeted in cancer to a higher extent than catalytic residues. Throughout evolution we observed that kinase specificity is strongly conserved across 1-to-1 orthologs but can diverge after gene duplication as illustrated by a reconstruction of the evolution of the G-protein coupled receptor kinase family. The identified SDRs can predict kinase specificity from sequence and aid in the interpretation of evolutionary or disease related genomic variants.

Introduction

Protein post-translational modifications (PTMs) constitute one of the fastest mechanisms of control of protein function. Among these, protein phosphorylation is the most extensive and well characterized PTM, with over 90,000 phosphosites discovered to date for human proteins alone (Lawrence et al., 2016). Protein kinases catalyse the phosphorylation of their target substrates, including other kinases, working in complex signalling networks that are capable of information processing and decision making. These signalling networks are involved in almost all cellular processes and mutations in protein kinases are often associated with disease (Brognard and Hunter, 2011; Lahiry et al., 2010; Stenberg et al., 2000). In addition, cross-species studies have shown that protein phosphorylation and kinase-substrate interactions can diverge at a very fast pace, suggesting that changes in post-translational control can be a driver of phenotypic diversity (Beltrao et al., 2009; Freschi et al., 2014; Studer et al., 2016). Understanding kinase signalling networks remains a difficult challenge, in particular because only a small fraction of the known phosphorylation sites can be assigned to their effector kinases.

There are 518 known human protein kinases (Manning et al., 2002), and their specificity of substrate recognition is shaped by the structural and chemical characteristics of both kinase and substrate (Ubersax and Ferrell, 2007). The general structure or fold of different kinases is quite similar and their specificity is, in part, determined by changes near the binding pocket. Kinases are thought to recognise a contiguous motif around the phosphosite (four/five amino acids on either side of the P-site) (Amanchy et al., 2007; Knighton et al., 1991; Pearson and Kemp, 1991; Pinna and Ruzzene, 1996) usually termed the kinase target motif. These target motif preferences are most often very degenerate with only a small number of key residues strongly contributing to the recognition. While these sequence preferences are thought to be important for target recognition, additional mechanisms contribute to specificity including: docking motifs; interaction with protein scaffolds; co-expression and co-localization (Biondi and Nebreda, 2003; Holland and Cooper, 1999). Sequence analysis has identified 9 kinase groups (AGC, CAMK, CMGC, RGC, TK, TKL, STE, CKI and other) but only a few kinase groups have clear differences in target preferences that are shared with most members of the group. For example the CMGC kinases tend to phosphorylate serine and threonine residues that have proline at position +1 relative to the phosphoacceptor (Kannan and Neuwald, 2004). However, for most kinase groups the preferences for residues around the target phosphoacceptor cannot be easily predicted from the primary sequence.

In previous studies of kinase specificity, the analysis of protein structures (Brinkworth et al., 2003; Saunders et al., 2008) and machine learning methods (Creixell et al., 2015a) have been used to identify positions within the kinase domain that determine kinase specificity – so called specificity determinant residues (SDRs). However, these approaches do not attempt to study the structural basis by which specific target preferences are determined. Methods based on comparative protein kinase alignments can achieve this, but have only been used to study a few kinase substrate preferences so far (Li et al.,2003; Kannan and Neuwald, 2004), or have been restricted to a single model organism (Mok et

al., 2010). Here we have combined alignment and structure based methods to identify and rationalize determinants of kinase specificity. We have identified SDRs for 16 target site preferences and show that these can be used to accurately predict kinase specificity. SDRs for two target preferences were further studied by mutagenesis and kinase activity assays. We provide detailed structural characterizations for many determinants and study how these are mutated in cancer or during evolution. Finally, we show how the knowledge of SDRs can be combined with ancestral sequence reconstruction to study the evolution of kinase specificity using as an example the G-protein coupled receptor kinase family.

Results

Identification of kinase specificity-determining residues and modelling of the kinase-substrate interface

To study kinase target preferences we compiled a list of 9005 experimentally validated and unique kinase-phosphosite relations for human, mouse and yeast kinases. Protein kinase specificities were modelled in the form of position probability matrices (PPMs) for 179 kinases, representing a fraction of the kinome of these species (human: 126/478, mouse: 35/504, *S. cerevisiae*: 18/116). For further analysis, we selected 135 high-confidence PPMs (87 human, 30 mouse, 18 yeast) that could successfully discriminate between target and non-target phosphorylation sites (see Methods). Throughout the text we may refer to the substrate amino-acids in single amino-acid letters and their position in the substrate relative to the target phosphoacceptor amino-acid (-5 to +5, where 0 is the target phosphoacceptor residue). For example, a proline residue at the +1 position may be abbreviated as P+1 or an arginine residue at the -3 position as R-3. For serine/threonine kinases, consistent evidence of active site selectivity is broadly apparent for the -3 and +1 positions relative to the phosphoacceptor amino-acid, and to a lesser extent the -2 position (**Figure 1a**). These constraints correspond mainly to the well-established preferences for basic side chains (arginine or lysine) at the -3 and/or -2 position, and in most CMGC kinases for proline at the +1 position. Tyrosine kinases however show little evidence of strong and consistent sequence constraint at the active site, and were excluded from further analysis as there were too few predictive PPMs (16) for the reliable detection of tyrosine kinase SDRs. These general trends only describe the most common modes of recognition shared across all kinases. Individual kinases can show preference for individual positions beyond these sites. All 135 high confidence kinase specificity models are summarized in **Supplementary Table 1**.

With the information on kinase specificities, we then attempted to understand more broadly the relationship between protein kinases and substrates at the active site by combining structural models (**Figure 1b**) and kinase sequence alignments (**Figure 1c**). We compiled 12 serine/threonine non-redundant experimental kinase models in complex with substrates in addition to 4 serine/threonine autophosphorylation complexes (Xu et al., 2015) (see full list in **Supplementary Table 2**). Kinase-substrate homology models for kinases of interest not present in this compilation of experimental models were also generated. A structural profile of substrate binding from position -5 to position +4 is given in **Supplementary**

Figure 1. The kinase positions most frequently in contact with the target peptide are highlighted also in **Figure 1b**. When referring to specific amino acids of the kinase, the single-letter code is used followed by the position of the residue based on the Pfam domain model that corresponds to the conserved catalytic domain (PF00069).

We developed a sequence alignment-based protocol for the automated detection of putative SDRs (**Methods, Figure 1c**). Briefly, the target preferences described as PPMs were clustered to identify groups of kinases with shared preferences at a position of interest. Putative SDRs are then inferred as those residues that discriminate all kinases with the common substrate preference (e.g. P+1) from those kinases without the same preference (**Figure 1c**). Using this approach we identified 30 positions that were predicted as SDRs for 16 preferences represented by more than 5 kinase PPMs (**Figure 2a**). These SDR positions are found across the whole sequence/structure of the kinase domain (**Figure 2b**) but not surprisingly cluster near the substrate-binding pocket (10 SDRs are within 4 Angstroms of the substrate peptide) **(Figure 2**c). Most of these determinants have not been described before and can be further studied by analysis of structural models. To assess the accuracy of these putative SDRs we tested if these could be used to predict the specificity of kinases from their sequence alone. For this we built sequence-based classifiers to predict the kinase specificity for the five preferences supported by at least 20 positive examples in the study dataset – P+1, P-2, R-2, R-3, and L-5. We used a cross-validation procedure where kinase sequences left out from the model training were later used for testing (**see Methods**). These models showed very strong performance with respective cross-validation tests, as measured by the area under the ROC curves: 0.99, 0.91, 0.82, 0.96, and 0.82 (**Supplementary figure 2**). This shows that, for these 5 specificities, the determinant residues can correctly predict the specificity of unseen kinases from their sequence alone, suggesting that the SDRs we have identified are broadly accurate.

Structural characterization of kinase SDRs

To further validate and study the putative SDRs we have used available co-crystal coordinates where possible. Models of relevant kinase-substrate complexes were alternatively generated using empirical complexes as a template (**see Methods**). Using these models we could suggest a structural rationale for SDRs of 8 target site preferences that are detailed in **Supplementary Figure 3**. These include the preferences for arginine at positions -3 and -2; proline at positions -2 and +1; leucine at positions +4 and -5 and for aspartate/glutamate at position +1 for AGC and CMGC kinases. Some of the SDRs have been previously identified in other studies underscoring the validity of our approach. For example, the specificity for proline at the +1 position is a well-studied preference and in our compilation it was found for 35 kinases of the CMGC group. Four of the six putative SDRs identified here map to the kinase pocket for the proline at the +1 position (**Supplementary Figure 3**) and match previously described determinants (Kannan and Neuwald, 2004) attesting to the accuracy of the methods used here.

We highlight in **Figure 3a** SDRs for 3 preferences that are less well studied: proline at position -2 (P-2) and leucine at positions +4 (L+4) and -5 (L-5). There are 25 kinases with a modest P-2 preference including MAPK1, CDK2, and DYRK1A. We identified 5 positions that are putative SDRs for P-2, two of which (161 and 162) are proximal to the residue in interaction models. In position 162, P-2 kinases usually contain a bulky hydrophobic residue (Y or W) not usually found in non- proline-directed kinases (**Supplementary Figure 3**). Both residues at these positions appear to form hydrophobic contacts with P-2 (**Figure 3a**). The domain position 161 was also implicated in the preference for the P+1 specificity mentioned above. The three other putative determinants – 82, 188, and 196 – are unlikely to be direct determinants given their distal position in the protein structure, although we note that 196 was implicated in a previous alignment-based study (Mok et al., 2010). These distal positions may influence the kinase preference through more complex mechanisms such as affecting the dynamics or conformation of the kinase.

We identified 21 kinases (14 CAMK; 5 AGC; 1 CMGC; 1 PRK) with a moderate L-5 preference. Positions 86 and 189 were predicted as determinants where L-5 kinases are marked by hydrophobic amino acids at position 86 and the absence of glutamate at 189. These residues can be observed to line the hydrophobic -5 position pocket of the MARK2 kinase (**Figure 3a**). Position 189 was also recently predicted to be an L-5 determinant from a comparative structural analysis of L-5 and R-5 kinases (Chen et al., 2017). For the leucine preference at the +4 position we identified six kinases - MARK2, CAMK1, PRKAA1, PRKAA2 (human), PRKAA1 (mouse), and Snf1 (yeast) - and the domain position 164 as the sole putative SDR. This residue is an alanine in five of the kinases listed above (valine in CAMK1). In the MARK2 cocrystal structure, the substrate peptide forms a turn at the +2 position so that the +4 hydrophobic side chain projects towards the kinase pocket of the +1 position and stacks against the +1 residue (**Figure 3a**). The substitution for alanine in place of residues with aliphatic side chains at position 164 in these kinases therefore seems to generate a small binding pocket that allows the L+4 to functionally substitute for the kinase position 164 by stacking against the +1 position.

We have selected two of the above described SDRs for experimental characterization (L-5 and L+4). To test these SDRs we performed kinase activity assays for SNF1 and two mutant versions: A218L (the 164 kinase position, an L+4 SDR) and V244R (the 189 kinase position, an L-5 SDR). These 3 kinases were separately incubated with a SNF1 target peptide of 15 amino acids that contains leucine at +4 and -5 as well as mutant versions with A+4 or D-5. The *in vitro* kinase reactions were stopped at 0, 2, 7 and 20 mins and the amount of phosphorylation was measured by mass spectrometry (Figure 3b and 3c). As predicted the A218L SNF1 showed an increased preference for the A+4 peptide but not for the D-5. The reverse was observed for the V244R SNF1 mutant. However, we noted that both mutant kinases showed a very strong decrease in overall kinase activity (Figure 3b). This could be due to either a potential destabilization of the kinase or a partial disruption of the activation mechanism by the two mutations.

The identification of previously known SDRs, the structural rationale for several of the novel SDRs and the experimental validation of two SDRs, further suggests that we have

here identified positions that are crucial for the recognition of kinases with specific preferences. The SDRs identified here can therefore be used to infer the specificity of other kinases from sequence and as we show below to study the consequences of mutations within the kinase domain.

Specificity determinant residues are often mutated in cancer

Some kinase SDRs have been observed to be mutated in cancer and congenital diseases (Berthon et al., 2015; Creixell et al., 2015b) and an enrichment of non-cancerous disease SNPs in regulatory and substrate-binding regions has previously been established (Dixit et al., 2009; Torkamani et al., 2008). Using mutation data from tumour patient samples from TCGA (http://cancergenome.nih.gov/), we have tested for the enrichment of tumour mutations in four categories of non-overlapping kinase residues: catalytic, regulatory, SDR (proximal to substrate), and 'other' (**Figure 4a**). Two of the five most commonly mutated residues are proximal to the primary activation loop phosphate. SDR residues close to the substrate show also a significant enrichment of mutations relative to 'other' residues (Wilcoxon p = 0.0017, **Figure 4b**). This enrichment is greater than that observed for catalytic and regulatory sites highlighting their functional relevance.

We next sought to determine if there was evidence of recurrent mutations mapping to the relevant SDRs of human kinases with a common peptide preference. Given that the specificity models only cover ~25% of all kinases we used the SDRs of the 5 most common preferences - P+1, P-2, R-2, R-3, and L-5 - to train sequence based predictors of kinase specificity as described above. Using these models we annotated all human kinases having a high probability for one of these specificities (**Supplementary Table 3**). We then compared the frequency of mutations per position for different kinase specificities and found significant differences in the relative mutation frequencies for kinase domain positions of the two most common preferences – P+1 and R-3 (represented in **Figure 4c**). Interestingly, domain position 164 and 161 of the +1 position loop exhibit high levels of differential mutation in the proline-directed kinases. For position 161, the MAP kinases in particular are recurrently mutated in independent samples (MAPK1: 3, MAPK8: 3, MAPK11: 2, MAPK1: 1).This position is known to bind to the phosphotyrosine at 157 that exists in MAPKs (Varjosalo et al., 2013). For the predicted R-3 kinases, the glycine 159 residue of the +1 position pocket is found to be commonly mutated, although this relates not to R-3 specificity *per se* but for +1 position binding of most non-CMGC kinases (Zhu et al., 2005). Residues 159 and 164 in particular are critical for specificity and highly conserved within the kinase subgroups, such that mutation to any other amino acid would be expected to abrogate +1 binding. These results suggest that there is a significant recurrence of cancer mutations targeting kinase specificity and not just kinase activity.

The work above illustrates how knowledge of the SDR residues is useful in understanding the functional consequences of cancer mutations. We next studied the changes in SDR residues during the evolution of protein kinases.

Evolution of G-protein coupled receptor kinase family specificity

The identification of the SDRs for specific target preferences allows us to study the evolution of kinase specificity. We first compared the changes in these residues across orthologs. We focused our analysis on the 5 specificities we can reliably predict from sequence as described above - P+1, P-2, R-2, R-3, and L-5. We observed that the five modelled preferences are highly conserved between orthologs, even for distantly related species. In P+1 kinases, for example, we predict divergence only for some fungal and plant orthologs of CDC20 but not for any other orthologs. For the 5 specificity classes and for *Arabidopsis thaliana* orthologs of human kinases we predict only 7 out of 245 (2.9%) cases where divergence of specificity is expected. These results show that orthologs most often have conserved specificities for hundreds of millions of years.

We then selected the GRK (G-protein coupled receptor kinase) kinase family as specific detailed case study of the evolution of target specificity. The GRK family is one of 15 families belonging to the AGC group (**Figure 5a)** (Manning et al., 2002). However, they have diverged from the characteristic basic residue preferences at positions -2/-5 and -3 of the AGC group (Lodowski et al., 2006). GRK2 for example is specific for aspartate/glutamate at position -3 (Lodowski et al., 2006; Onorato et al., 1991), and in the GRK5 model presented here the R-3 signature is absent (**Figure 5b**). The GRK family is divided into the BARK (β-adrenergic receptor kinase) subfamily – comprising GRK2 (ADRBK1) and GRK3 (ADRBK2) in human – and the GRK subfamily -- comprising GRK1 (rhodopsin kinase), GRK4, GRK5, GRK6, and GRK7. We have taken a taxonomically broad sample of 163 GRK kinase sequences to generate a comprehensive phylogeny (**Figure 5a**, Methods). From this, a maximum-likelihood reconstruction of ancestral sequence states has been performed (Methods) in order to study the evolution of substrate preferences on the basis of our detailed understanding of kinase SDRs.

The topology of the tree is in general agreement with a previously published GRK phylogeny (Mushegian et al., 2012). Focusing on the specificity at the -2 and -3 positions (**Figure 5c and Supplementary Figure 4**), two substitutions between the ancestor of RSK and GRK kinases and the ancestor of all GRK kinases likely caused a reduced preference for arginine at -3 and -2 positions. The substitution of glutamate for glycine at position 162 – an R-3 and R-2 determinant (**Supplementary Figure 3**) -- and the substitution of phenylalanine at position 86 – most likely either to histidine or to lysine. From this ancestral node towards the Rhizarian lineage an additional substitution of glutamate at 189 for arginine likely drove the complete switch from R-2/R-3 to a novel aspartate/glutamate preference at the -2 position. This 86K/189R pair is analogous to the 127E/189E pair found in basophilic kinases. In the heterokont lineages, the histidine/lysine at position 86 in the ancestror of GRK kinases was substituted for serine and while these kinases retained the 86E/189E pair, the R-2 and R-3 specificities are likely to be attenuated or eliminated given the substitutions at 86 and 162. The BARK kinases had two charge altering substitutions -- E127A and E189K – that likely caused the preference for aspartate/glutamate at the -2 and -3 positions as observed today in GRK2 (**Figure 5b**). Finally, in the GRK subfamily, a lysine residue (or arginine in GRK1) is usually found at position 86. Notably, no R-2/R-3/R-

5 preference is evident for GRK5 (**Figure 5b**), suggesting that the described substitutions (E162G and E189K) are sufficient to eliminate this specificity.

The GRK family illustrates how the target preference of a kinase can change after kinase duplication via the substitution of a few key residues. It also illustrates one example where distantly-related kinase orthologs may have diverged when comparing the metazoan GRKs to their rhizaria homologs that diverged around 1700 million years ago (Kumar et al., 2017).

Discussion

We have here addressed the challenge of identifying which residues determine kinase preferences towards specific amino-acids at specific positions around the target phosphosite. Initial studies of kinase determinants used structures of kinases in complex with target peptides to identify SDR residues as those important for substrate binding (Brinkworth et al., 2003; Zhu et al., 2005). A more recent work has used a machine learning approach to identify SDR residues as those that globally maximized the specificity predictive power (Creixell et al., 2015a). These approaches have identified SDR positions but do not assign positions and residues according to specific target preferences (e.g. R-3 or P+1). Alternatively, alignment-based approaches can be used to identify residues that contribute to particular preferences but so far have been restricted to a few kinase groups (Li et al., 2003; Kannan and Neuwald, 2004), or have lacked structural characterization (Mok et al., 2010). Here we have combined a statistical analysis of known kinase targets with alignment and structure based approaches to identify and study SDRs. The primary goal of this study was to identify and rationalize SDRs for particular preferences. Importantly, our analyses clearly show how different positions contribute in unique ways to target site recognition. Many SDR positions were found distal to the substrate binding site. These are harder to rationalize structurally and additional work will need to be done to establish how they relate to target site preference. The SNF1 mutations of SDRs validated two positions contributing to the expected target preferences but also showed a very drastic reduction in activity. This reduction in activity could be due to destabilization of the kinase or a partial disruption of the kinase activation mechanism. Additional mutant studies would be needed to characterize the interplay between activity and specificity and the mutational trajectories that allow for specificity switching.

The study of cancer mutations has revealed that SDRs are commonly mutated as shown previously (Creixell et al., 2015b). In addition to previous studies, we observed that SDR mutation burden in cancer can reflect kinase specificities with specific residues being targeted depending on the kinase preferences. These SDR mutations may still have a large impact on the kinase activity as was the case for the SNF1 SDR mutants, perhaps by interfering with the activation mechanism of these kinases. Understanding the impact of mutations in kinases will facilitate the classification of cancer mutations into drivers or passenger depending on their functional consequences. Our results suggest that grouping all SDR positions regardless of the kinase specificity will tend to overestimate the impact of mutations since many SDR positions are only relevant for one or few specificities.

The identification of the SDRs allows us to study the evolution of kinase preferences by ancestral sequence reconstruction. The protein kinase domain has been extensively duplicated throughout evolution but very little is known about the process of divergence of kinase target preference. Our results strongly suggest that kinase orthologs tend to maintain their specificity. This would be expected as they can regulate up to hundreds of targets (Imamura *et al.,* 2014; Manning and Cantley, 2007) and a change in specificity would drastically alter the regulation of a large number of proteins. This high conservation of kinase specificity contrasts to the larger divergence rate of kinase target sites (Beltrao et al., 2009; Freschi et al., 2014; Studer et al., 2016). The fast evolutionary plasticity of kinase signaling therefore relies primarily on the turnover of target sites that can occur without the need for gene duplication.

Divergence of specificity within kinase families is more likely to occur after gene duplication. A previous study has shown how the Ime2 kinases (RCK family) have diverged from the other CMGC kinases in their typical preference for proline at the +1 position (Howard et al., 2014). Here we have traced the putative evolutionary history of the GRK family preference at the -2/-3 positions, which illustrate a divergence of kinase specificity between paralogs and also distantly-related orthologs. An understanding of kinase SDRs will allow for further studies of how the variety of target peptide preferences has come about during evolution and the rate at which kinase can switch their preferences after gene duplication.

Kinase target recognition within the cell is complex and the specificity at the active site is only one of several mechanisms that can determine kinase-substrate interactions (Ubersax and Ferrell, 2007). Much additional work is needed to establish a global comprehensive view of kinase target specificity and its evolution.

Methods

Kinase specificity models

Known kinase target phosphosites for human, mouse and *S. cerevisiae* were retrieved from HPRD, PhosphoSitePlus, Phospho.ELM and PhosphoGRID (Dinkel et al., 2011; Hornbeck et al., 2015; Prasad et al., 2009; Sadowski et al., 2013). PhosphoGRID target sites supported exclusively by kinase perturbation followed by MS were excluded and homologous sequences above 85% identity were removed with CD-HIT (Li and Godzik, 2006). Phosphosites mapping to the kinase activation segment were also removed as kinase autophosphorylation sites often conform poorly to kinase consensus motifs (Miller et al., 2008; Pike et al., 2008). Specificity matrices for each kinase with at least ten target sites were constructed in the form of a position probability matrix (PPM) - 20 x 11 matrices with the columns representing substrate positions -5 to +5; each value representing the empirical residue frequencies for a given amino-acid at a substrate position. For the purpose of scoring only, the PPMs were converted into PWMs by accounting for background amino acid frequencies in the proteome. Cross-validation was used to assess kinase model performance and PWMs with an average area under the curve (AUC) value < 0.6 were excluded from further analysis. Too few tyrosine kinase PPMs remained after

these filtering steps and we excluded them for further analysis. Kinase group/family/subfamily classifications were based on the KinBase data resource unless otherwise specified (Manning et al., 2002).

Position-based clustering of specificity models and sequence alignment-based detection of putative specificity determining residues (SDRs).

Clustering of the PPMs was performed in a position-based manner for each of the five sites N- and C-terminal to the phosphoacceptor amino acid (-5, -4, -3, -2, -1; +1, +2, +3, +4, +5) using the affinity propagation (AP) algorithm (Frey and Dueck, 2007) as implemented in the APCluster R package (Bodenhofer et al., 2011). Non-specific clusters or clusters with fewer than 6 constituent kinases were excluded and the clusters were further modified to account for potential false positive and false negative cases (see extended Supplementary Methods). The MAFFT L-INS-i method was used to generate kinase MSAs for this analysis (Katoh et al., 2005) and the *trim*Al tool was used remove MSA positions containing more than 20% 'gap' sites (Capella-Gutiérrez et al., 2009). Kinases were then grouped by specificity according to the clustering of their specificity models, as described above, and then iteratively we predicted SDRs for each cluster (e. g. preference for proline at +1 position). To identify putative SDRs, three high-performing methods alignment-based methods were selected (GroupSim, Multi-Relief 3D, SPEER) from previous benchmarking tests (Chakraborty and Chakrabarti, 2015). Incorporating predictions from the three methods is expected to achieve higher specificity than any single method (Chakrabarti and Panchenko, 2009). As the GroupSim, Multi-Relief 3D, and SPEER methods use distinct schemes for position scoring we selected as putative SDRs those residues lying within a three-way intersection of the top 15 ranked sites for the single methods, as proposed by *Chakrabarti and Panchenko 2009*.

Kinase-substrate structures

Empirical kinase structures alone and in complex with putative target sequences were retrieved from the PDB (see extended Supplementary Methods). An automated procedure was implemented to identify the kinase substrate-binding residues for the substrate positions -5 to +4 (excluding P0) and all binding residues contacts were categorised as either hydrogen-bonded, ionic, or non-bonded (i.e. hydrophobic or van der Waals). Kinase-substrate homology models were constructed by first superposing the kinase of interest (query) with a template cocrystal structure to achieve a plausible positioning of the substrate peptide. The template kinase were removed and the template peptide mutated *in Silico* (using FoldX (Schymkowitz et al., 2005)) to the sequence of a known phosphorylation site of the query kinase. After resolving steric clashes between kinase and substrate, the resulting complexes were then subjected to energy minimisation (EM), followed by molecular dynamics (MD) equilibration and production runs using NAMD (Phillips et al., 2005) (see extended Supplementary Methods for additional details).

Construction of predictive models, cross-validation, and orthology analysis

Naive Bayes (NB) algorithms were used to predict the specificity of protein kinases on the basis of sequence alone. Five separate classifiers were generated, corresponding to the

five preferences -- P+1, P-2, R-2, R-3, and L-5 -- supported by at least 20 kinases. Each classifier was trained on the 119 Ser/Thr kinase sequences of known specificity, where each kinase was labelled ('positive' or 'negative') according to the clustering of kinase specificity models described above. Leave one-out cross-validation (LOOCV) was then used for each classifier to identify the subset of input SDRs that would optimise the performance of the model on the training data with respect to the AUC. The R libraries *klaR* and *cvTools* were used for model generation and cross-validation, respectively (Alfons, 2012; Weihs et al., 2005). For the analysis of protein kinase orthologs, orthologous kinase sequences were retrieved automatically from the Ensembl Genomes database (Kersey et al., 2015) using the Ensembl Rest API and were aligned using the MAFFT L-INS-i method. Each sequence was then queried with the specificity model corresponding to the known specificity of the human ortholog.

Analysis of kinase mutations in cancer

Mutation data for primary tumour samples was obtained from The Cancer Genome Atlas (TCGA) (http://cancergenome.nih.gov/). Each kinase mutation was assigned to the correct protein isoform and then mapped to the corresponding kinase domain position. All kinase domain positions were categorised as 'SDR', 'Catalytic', 'Regulatory', and 'Other'. Catalytic and regulatory sites were inferred from the literature. 'SDR' sites refers to residues that are both potential SDRs (Figure 2a) and often found in close contact with the substrate peptide (Figure 1b). 'Other' refers to the complement of these three sets relative to the kinase domain. Exact positions are defined in extended Supplementary Methods.

GRK phylogeny and ancestral sequence reconstruction

Protein sequences were retrieved from a taxonomically-broad set of non-redundant proteomes (representative proteomes) (Chen et al., 2011), and then each representative proteome (rp35) was queried with a hidden Markov model (HMM) of the GRK domain (KinBase) using *HMMsearch* (E = 1e-75) *(Eddy, 1998)*. The subfamily classifications of each GRK were then predicted using Kinannote (Goldberg et al., 2013). Sample sequences of the RSK family kinases – the family most similar in sequence to the GRKs – were also included as an expected outgroup in the phylogeny, as were two kinases of the basophilic PKA family. The kinase sequences (GRK kinases plus outgroups) were then aligned using the L-INS-i algorithm of MAFFT (Katoh and Standley, 2013), and filtered to remove pseudokinases and redundant sequences (97% threshold), resulting in 163 sequences to be used for phylogenetic reconstruction. A maximum likelihood phylogeny was generated with RAxML using a gamma model to account for the heterogeneity of rates between sites. The optimum substitution matrix (LG) for reconstruction was also determined with RAxML using a likelihood-based approach (Stamatakis, 2014). FastML was then used for the ML-based ancestral reconstruction of sequences for all nodes in the phylogeny (Ashkenazy et al., 2012). Sequence probabilities were calculated marginally using a gamma rate model and the LG substitution matrix.

SNF1 mutant *in vitro* kinase activity assay

The SNF1 plasmid from the Yeast Gal ORF collection was used as a template for directed mutagenesis to create the mutants A218L and V244R. Wild type and mutant plasmids

were transformed into a BY4741 SNF1 KO strain. Cells were grown to exponential phase in SD media lacking uracil, and Snf1 expression was induced with 2% galactose for 8h. Cell pellets were collected, lysed using protease and phosphates inhibitors (Sigma) and stored O/N at -80C. Snf1 immunoprecipitation was performed using Protein A agarose beads (Sigma) with rotation for 2h at 4C. Kinase assay was performed using AQUA synthetic peptides (Sigma). Each of the 3 kinases was incubated with equal concentration of the 3 synthetic peptides (VQLKRPASVLALNDL, VQDKRPASVLALNDL and VQLKRPASVLAANDL), ATP mix (ATP 300 µM, 15 mM MgCl2, 0.5 mM EGTA, 15 mM β-glycerol phosphate, 0.2 mM sodium orthovanadate, 0.3 mM DTT) and allowed to react for 0, 2, 7 and 20 minutes. The reactions were quenched by transferring the reaction mixture onto dry ice at the corresponding times.

Mass spectrometry identification and quantification

Kinase reaction products were diluted with 0.1% formic acid in LC-MS grade water and 5 µl of solution (containing 10 pmol of the unmodified peptide substrates) were loaded LC-MS/MS system consisting of a nanoflow ultimate 3000 RSL nano instrument coupled on-line to a Q-Exactive Plus mass spectrometer (Thermo Fisher Scientific). Gradient elution was from 3% to 35% buffer B in 15 min at a flow rate 250 nL/min with buffer A being used to balance the mobile phase (buffer A was 0.1% formic acid in LC-MS grade water and B was 0.1% formic acid in LC-MS grade acetonitrile). The mass spectrometer was controlled by Xcalibur software (version 4.0) and operated in the positive ion mode. The spray voltage was 2 kV and the capillary temperature was set to 255 ºC. The Q-Exactive Plus was operated in data dependent mode with one survey MS scan followed by 15 MS/MS scans. The full scans were acquired in the mass analyser at 375- 1500m/z with the resolution of 70 000, and the MS/MS scans were obtained with a resolution of 17 500. For quantification of each phosphopeptide and its respective unmodified form, the extracted ion chromatograms were integrated using the theoretical masses of ions using a mass tolerance of 5 ppm. Values of area-under-the-curve were obtained manually in Qual browser of Xcalibur software (version 4.0).

Figures

Figure 1 - a) Sequence constraint for substrate positions -5 to +5 for 119 serine/threonine kinases, measured as the bit value for the corresponding column of the kinase PSSM. b) Interface between a protein kinase (human protein kinase A) and substrate peptide at the substrate-binding site. Kinase residues that commonly bind the substrate peptide (yellow) are represented in stick format and coloured according to the corresponding substrate position (-3: red, -2: pink, -1: orange, +1: green, +2: blue, +3: purple). Residue numbering represents the relevant positions of the Pfam protein kinase domain (PF00069) c) Semi-automated pipeline for the inference of putative kinase SDRs (specificity-determining residues). The first step involves the construction of many kinase PPMs from known target phosphorylation sites. Vectors corresponding to a substrate position of interest (e.g. +1) are then retrieved from each PPM. An unsupervised learning approach (i.e. clustering) then identifies kinases with a common position-based preference (e.g. for proline at P+1). Alignment positions that best discriminate kinases belonging to one cluster from all others are then identified using automated tools for SDR detection.

Figure 2 - Position of identified SDRs along the kinase sequence and structure. All putative kinase SDRs from our analysis are a) listed in a table with their corresponding position preferences b) mapped to a 1D representation of the kinase secondary structure c) mapped to a kinase-substrate complex structure (PDB: 1atp). The SDRs colored in dark red b) and c) represent positions within 4 Angstroms of the substrate peptide.

Figure 3 - Structural rationale for kinase SDRs and validation experiments. a) Kinase-substrate interface for:proline at position -2 (PDB: 2wo6), leucine at position -5 (PDB: 3iec) and leucine at position +4 (PDB: 3iec). The substrate peptides are colored in yellow, and putative SDRs in red. A structural rationalisation for each preference is provided briefly in the main text 'Structural characterization of kinase SDRs', and in more detail in **Supplementary Figure 3**. b) Kinase activity assays for SNF1 WT and two mutant versions A218L (the 164 kinase position, an L+4 SDR) and V244R (the 189 kinase position, an L-5 SDR). The 3 kinases were incubated separately with a known SNF1 target peptide with L at +4 and -5 (orange) as well as the mutant versions A+5 (green) and D-5 (blue). Replicates of *in vitro* reactions were quenched at 0, 2, 7 and 20 mins and the amount of phosphorylation was measured by mass spectrometry. c) Average and standard deviation of phosphopetide intensity per time (for time points 2, 7 and 20 mins combined).

Figure 4 - SDRs are often mutated in cancer. a) Kinase domain positions are colored according to their functional category (regulatory: orange, catalytic: blue, SDR: red, 'other': grey). The substrate peptide is represented in yellow and ATP in green, orange, and red. b) The fraction of mutations mapping to a given site for a given kinase were calculated, and then averaged across all kinases. The different sites are grouped according to their functional category. c) For a given site, the frequency of mutations in arginine-3 kinases (x-axis) and proline+1 kinases (y-axis) is plotted. Putative SDRs are colored in red.

Figure 5 - Evolution of GRK family specificity. a) Phylogeny of kinases in the GRK family, including an outgroup of RSK kinases in human. The supporting number of bootstrap replicates (/100) for relevant clades and bifurcations is represented. b) Logos at positions -3 and -2 for human RSPS6KA1 (RSK kinase), human GRK2 (GRK/BARK kinase), and human GRK5 (GRK/GRK kinase). Sequence logos were generated from target phosphorylation sites. c) Representation of substrate position -2 and -3 (yellow), and their corresponding kinase binding pockets (cyan) for extant kinases and predicted ancestral sequences. Substitutions in the binding pocket are denoted by a red asterisk.

References

Alfons, A. (2012). cvTools: Cross-validation tools for regression models. R Package Version 0. 3 *2*.

Amanchy, R., Periaswamy, B., Mathivanan, S., Reddy, R., Tattikota, S.G., and Pandey, A. (2007). A curated compendium of phosphorylation motifs. Nat. Biotechnol. *25*, 285–286.

Ashkenazy, H., Penn, O., Doron-Faigenboim, A., Cohen, O., Cannarozzi, G., Zomer, O., and Pupko, T. (2012). FastML: a web server for probabilistic reconstruction of ancestral sequences. Nucleic Acids Res. *40*, W580–W584.

Beltrao, P., Trinidad, J.C., Fiedler, D., Roguev, A., Lim, W.A., Shokat, K.M., Burlingame, A.L., and Krogan, N.J. (2009). Evolution of phosphoregulation: comparison of phosphorylation patterns across yeast species. PLoS Biol. *7*, e1000134.

Berthon, A.S., Szarek, E., and Stratakis, C.A. (2015). PRKACA: the catalytic subunit of protein kinase A and adrenocortical tumors. Front Cell Dev Biol *3*, 26.

Biondi, R.M., and Nebreda, A.R. (2003). Signalling specificity of Ser/Thr protein kinases through docking-site-mediated interactions. Biochem. J *372*, 1–13.

Bodenhofer, U., Kothmeier, A., and Hochreiter, S. (2011). APCluster: an R package for affinity propagation clustering. Bioinformatics *27*, 2463–2464.

Brinkworth, R.I., Breinl, R.A., and Kobe, B. (2003). Structural basis and prediction of substrate specificity in protein serine/threonine kinases. Proc. Natl. Acad. Sci. U. S. A. *100*, 74–79.

Brognard, J., and Hunter, T. (2011). Protein kinase signaling networks in cancer. Curr. Opin. Genet. Dev. *21*, 4–11.

Capella-Gutiérrez, S., Silla-Martínez, J.M., and Gabaldón, T. (2009). trimAl: a tool for automated alignment trimming in large-scale phylogenetic analyses. Bioinformatics *25*, 1972–1973.

Chakrabarti, S., and Panchenko, A.R. (2009). Ensemble approach to predict specificity determinants: benchmarking and validation. BMC Bioinformatics *10*, 207.

Chakraborty, A., and Chakrabarti, S. (2015). A survey on prediction of specificity-determining sites in proteins. Brief. Bioinform. *16*, 71–88.

Chen, C., Natale, D.A., Finn, R.D., Huang, H., Zhang, J., Wu, C.H., and Mazumder, R. (2011). Representative proteomes: a stable, scalable and unbiased proteome set for sequence analysis and functional annotation. PLoS One *6*, e18910.

Chen, C., Nimlamool, W., Miller, C.J., Lou, H.J., and Turk, B.E. (2017). Rational Redesign of a Functional Protein Kinase-Substrate Interaction. ACS Chem. Biol. *12*, 1194–1198.

Creixell, P., Palmeri, A., Miller, C.J., Lou, H.J., Santini, C.C., Nielsen, M., Turk, B.E., and Linding, R. (2015a). Unmasking determinants of specificity in the human kinome. Cell *163*, 187–201.

Creixell, P., Schoof, E.M., Simpson, C.D., Longden, J., Miller, C.J., Lou, H.J., Perryman, L., Cox, T.R., Zivanovic, N., Palmeri, A., et al. (2015b). Kinome-wide decoding of network-attacking mutations rewiring cancer signaling. Cell *163*, 202–217.

Dinkel, H., Chica, C., Via, A., Gould, C.M., Jensen, L.J., Gibson, T.J., and Diella, F. (2011). Phospho.ELM: a database of phosphorylation sites—update 2011. Nucleic Acids Res. *39*, D261–D267.

Dixit, A., Yi, L., Gowthaman, R., Torkamani, A., Schork, N.J., and Verkhivker, G.M. (2009). Sequence and structure signatures of cancer mutation hotspots in protein kinases. PLoS One *4*, e7485.

Eddy, S.R. (1998). Profile hidden Markov models. Bioinformatics *14*, 755–763.

Freschi, L., Osseni, M., and Landry, C.R. (2014). Functional divergence and evolutionary turnover in mammalian phosphoproteomes. PLoS Genet. *10*, e1004062.

Frey, B.J., and Dueck, D. (2007). Clustering by passing messages between data points. Science *315*, 972–976.

Goldberg, J.M., Griggs, A.D., Smith, J.L., Haas, B.J., Wortman, J.R., and Zeng, Q. (2013). Kinannote, a computer program to identify and classify members of the eukaryotic protein kinase superfamily. Bioinformatics *29*, 2387–2394.

Holland, P.M., and Cooper, J.A. (1999). Protein modification: docking sites for kinases. Curr. Biol. *9*, R329–R331.

Hornbeck, P.V., Zhang, B., Murray, B., Kornhauser, J.M., Latham, V., and Skrzypek, E. (2015). PhosphoSitePlus, 2014: mutations, PTMs and recalibrations. Nucleic Acids Res. *43*, D512–D520.

Howard, C.J., Hanson-Smith, V., Kennedy, K.J., Miller, C.J., Lou, H.J., Johnson, A.D., Turk, B.E., and Holt, L.J. (2014). Ancestral resurrection reveals evolutionary mechanisms of kinase plasticity. Elife *3*.

Kannan, N., and Neuwald, A.F. (2004). Evolutionary constraints associated with functional specificity of the CMGC protein kinases MAPK, CDK, GSK, SRPK, DYRK, and CK2α. Protein Sci. *13*, 2059–2077.

Katoh, K., and Standley, D.M. (2013). MAFFT multiple sequence alignment software version 7: improvements in performance and usability. Mol. Biol. Evol. *30*, 772–780.

Katoh, K., Kuma, K.-I., Toh, H., and Miyata, T. (2005). MAFFT version 5: improvement in accuracy of multiple sequence alignment. Nucleic Acids Res. *33*, 511–518.

Kersey, P.J., Allen, J.E., Armean, I., Boddu, S., Bolt, B.J., Carvalho-Silva, D., Christensen, M., Davis, P., Falin, L.J., Grabmueller, C., et al. (2016). Ensembl Genomes 2016: more genomes, more complexity. Nucleic Acids Res. *44*, D574-580.

Knighton, D.R., Zheng, J.H., Ten Eyck, L.F., Ashford, V.A., Xuong, N.H., Taylor, S.S., and Sowadski, J.M. (1991). Crystal structure of the catalytic subunit of cyclic adenosine monophosphate-dependent protein kinase. Science *253*, 407–414.

Kumar, S., Stecher, G., Suleski, M., and Hedges, S.B. (2017). TimeTree: A Resource for Timelines, Timetrees, and Divergence Times. Mol. Biol. Evol. *34*, 1812–1819.

Lahiry, P., Torkamani, A., Schork, N.J., and Hegele, R.A. (2010). Kinase mutations in human disease: interpreting genotype-phenotype relationships. Nat. Rev. Genet. *11*, 60–74.

Lawrence, R.T., Searle. B.C., Llovet, A, Villen, J. (2016). Plug-and-Play analysis of the human phosphoproteome by targeted high-resolution mass spectrometry. Nat Methods. *13*, 431-434

Li, L., Shakhnovich, E.I., Mirny, L.A. (2003). Amino acids determining enzyme-substrate specificity in prokaryotic and eukaryotic protein kinases. Proc. Natl. Acad. Sci. U. S. A. *15*, 4463-4468.

Lodowski, D.T., Tesmer, V.M., Benovic, J.L., and Tesmer, J.J.G. (2006). The structure of G protein-coupled receptor kinase (GRK)-6 defines a second lineage of GRKs. J. Biol. Chem. *281*, 16785–16793.

Manning, G., Whyte, D.B., Martinez, R., Hunter, T., and Sudarsanam, S. (2002). The protein kinase complement of the human genome. Science *298*, 1912–1934.

Miller, M.L., Jensen, L.J., Diella, F., Jørgensen, C., Tinti, M., Li, L., Hsiung, M., Parker, S.A., Bordeaux, J., Sicheritz-Ponten, T., et al. (2008). Linear motif atlas for phosphorylation-dependent signaling. Sci. Signal. *1*, ra2.

Mok, J., Kim, P.M., Lam, H.Y.K., Piccirillo, S., Zhou, X., Jeschke, G.R., Sheridan, D.L., Parker, S.A., Desai, V., Jwa, M., et al. (2010). Deciphering protein kinase specificity through large-scale analysis of yeast phosphorylation site motifs. Sci. Signal. *3*, ra12.

Mushegian, A., Gurevich, V.V., and Gurevich, E.V. (2012). The origin and evolution of G protein-coupled receptor kinases. PLoS One *7*, e33806.

Onorato, J.J., Palczewski, K., Regan, J.W., Caron, M.G., Lefkowitz, R.J., and Benovic, J.L. (1991). Role of acidic amino acids in peptide substrates of the beta-adrenergic receptor kinase and rhodopsin kinase. Biochemistry *30*, 5118–5125.

Pearson, R.B., and Kemp, B.E. (1991). Protein kinase phosphorylation site sequences and consensus specificity motifs: tabulations. Methods Enzymol. *200*, 62–81.

Phillips, J.C., Braun, R., Wang, W., Gumbart, J., Tajkhorshid, E., Villa, E., Chipot, C., Skeel, R.D., Kalé, L., and Schulten, K. (2005). Scalable molecular dynamics with NAMD. J. Comput. Chem. *26*, 1781–1802.

Pike, A.C.W., Rellos, P., Niesen, F.H., Turnbull, A., Oliver, A.W., Parker, S.A., Turk, B.E., Pearl, L.H., and Knapp, S. (2008). Activation segment dimerization: a mechanism for kinase autophosphorylation of non consensus sites. EMBO J. *27*, 704–714.

Pinna, L.A., and Ruzzene, M. (1996). How do protein kinases recognize their substrates? Biochim. Biophys. Acta *1314*, 191–225.

Prasad, T.S.K., Kandasamy, K., and Pandey, A. (2009). Human Protein Reference Database and Human Proteinpedia as discovery tools for systems biology. Methods Mol. Biol. *577*, 67–79.

Sadowski, I., Breitkreutz, B.-J., Stark, C., Su, T.-C., Dahabieh, M., Raithatha, S., Bernhard, W., Oughtred, R., Dolinski, K., Barreto, K., et al. (2013). The PhosphoGRID Saccharomyces cerevisiae protein phosphorylation site database: version 2.0 update. Database *2013*, bat026.

Saunders, N.F.W., Brinkworth, R.I., Huber, T., Kemp, B.E., and Kobe, B. (2008). Predikin and PredikinDB: a computational framework for the prediction of protein kinase peptide specificity and an associated database of phosphorylation sites. BMC Bioinformatics *9*, 245.

Schymkowitz, J.W.H., Rousseau, F., Martins, I.C., Ferkinghoff-Borg, J., Stricher, F., and Serrano, L. (2005). Prediction of water and metal binding sites and their affinities by using the Fold-X force field. Proc. Natl. Acad. Sci. U. S. A. *102*, 10147–10152.

Stamatakis, A. (2014). RAxML version 8: a tool for phylogenetic analysis and post-analysis of large phylogenies. Bioinformatics *30*, 1312–1313.

Stenberg, K.A., Riikonen, P.T., and Vihinen, M. (2000). KinMutBase, a database of human disease-causing protein kinase mutations. Nucleic Acids Res. *28*, 369–371.

Studer, R.A., Rodriguez-Mias, R.A., Haas, K.M., Hsu, J.I., Viéitez, C., Solé, C., Swaney, D.L., Stanford, L.B., Liachko, I., Böttcher, R., et al. (2016). Evolution of protein phosphorylation across 18 fungal species. Science *354*, 229–232.

Torkamani, A., Kannan, N., Taylor, S.S., and Schork, N.J. (2008). Congenital disease SNPs target lineage specific structural elements in protein kinases. Proc. Natl. Acad. Sci. U. S. A. *105*, 9011–9016.

Ubersax, J.A., and Ferrell, J.E., Jr (2007). Mechanisms of specificity in protein phosphorylation. Nat. Rev. Mol. Cell Biol. *8*, 530–541.

Varjosalo, M., Keskitalo, S., Van Drogen, A., Nurkkala, H., Vichalkovski, A., Aebersold, R., and Gstaiger, M. (2013). The protein interaction landscape of the human CMGC kinase group. Cell Rep. *3*, 1306–1320.

Weihs, C., Ligges, U., Luebke, K., and Raabe, N. (2005). klaR Analyzing German Business Cycles. In Data Analysis and Decision Support, (Springer, Berlin, Heidelberg), pp. 335–343.

Xu, Q., Malecka, K.L., Fink, L., Jordan, E.J., Duffy, E., Kolander, S., Peterson, J.R., and Dunbrack, R.L., Jr (2015). Identifying three-dimensional structures of autophosphorylation complexes in crystals of protein kinases. Sci. Signal. *8*, rs13.

Zhu, G., Fujii, K., Belkina, N., Liu, Y., James, M., Herrero, J., and Shaw, S. (2005). Exceptional disfavor for proline at the P+ 1 position among AGC and CAMK kinases establishes reciprocal specificity between them and the proline-directed kinases. J. Biol. Chem. *280*, 10743–10748.

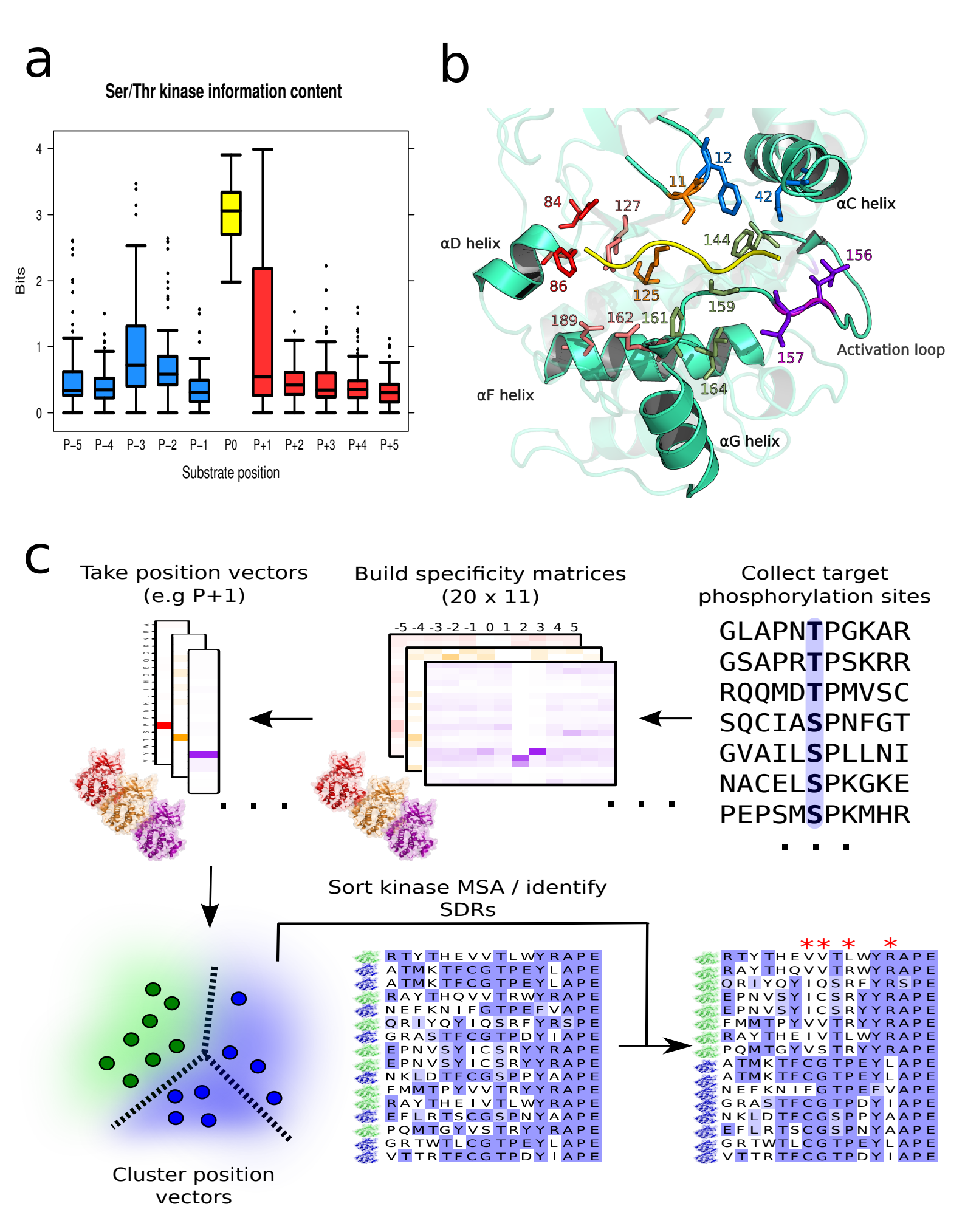
a
Ser/Thr kinase information content
Bits
Substrate position
P–5
P–4
P–3
P–2
P–1
P0
P+1
P+2
P+3
P+4
P+5
b
αC helix
αD helix
αF helix
αG helix
Activation loop
c
Take position vectors
(e.g P+1)
Build specificity matrices
(20 x 11)
Collect target
phosphorylation sites
GLAPNTPGKAR
GSAPRTPSKRR
RQQMDTPMVSC
SQCIASPNFGT
GVAILSPLLNI
NACELSPKGKE
PEPSMSPKMHR
Sort kinase MSA / identify
SDRs
Cluster position
vectors

a

Preference	SDR positions
Arg-3 (55)	17, 82, 86, 127, 158, 162, 185
Pro+ 1 (36)	158, 159, 161, 164, 188, 196
Arg-2 (27)	27, 162
Pro-2 (25)	82, 161, 162, 188, 196
Leu-5 (21)	86, 189
Arg/ lys+ 2 (14)	45, 61, 126, 229
Asp/ glu-2 (13)	157, 189
Asp/ glu-3 (13)	86, 127, 140, 157
Arg-5 (12)	162
Arg/ lys+ 3 (10)	161, 237
Arg-5 (12)	162
Asp/ glu+ 1	85, 249
Leu-2 (8)	131
Asp/ glu+ 2 (7)	13, 34
Pro+ 2 (7)	145
Leu+ 4 (6)	164
Asp/ glu+ 4 (6)	73, 142, 165, 249

c

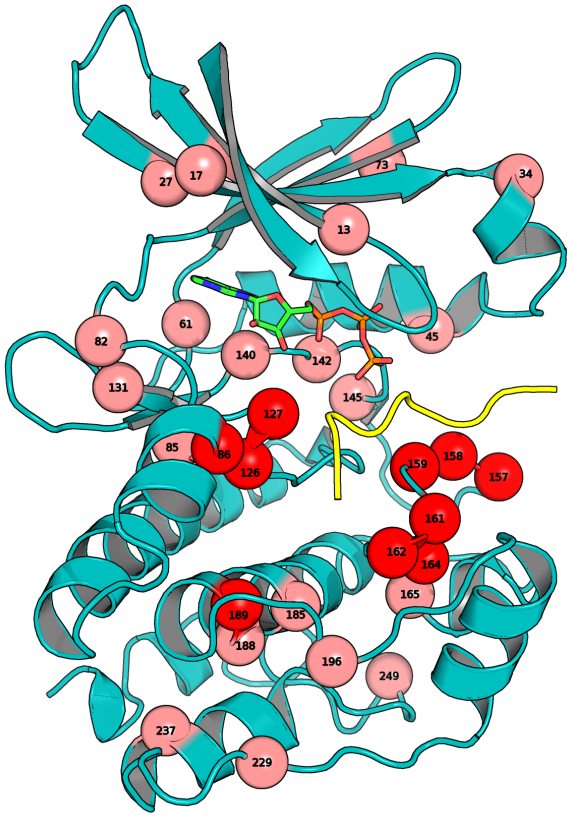

b

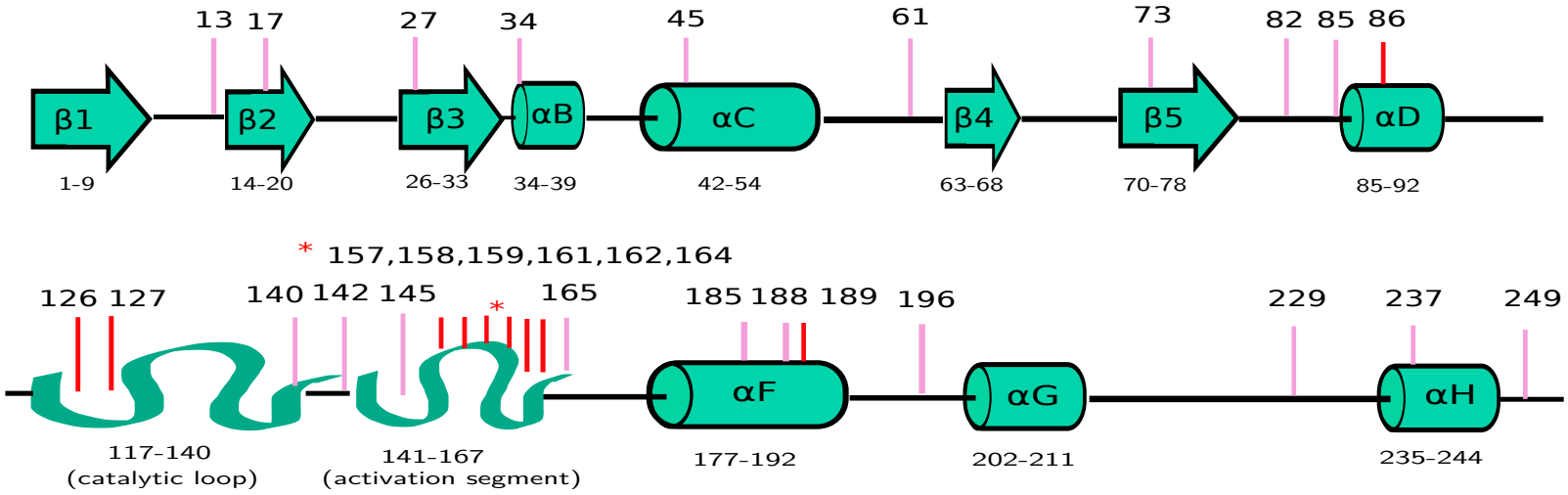

a

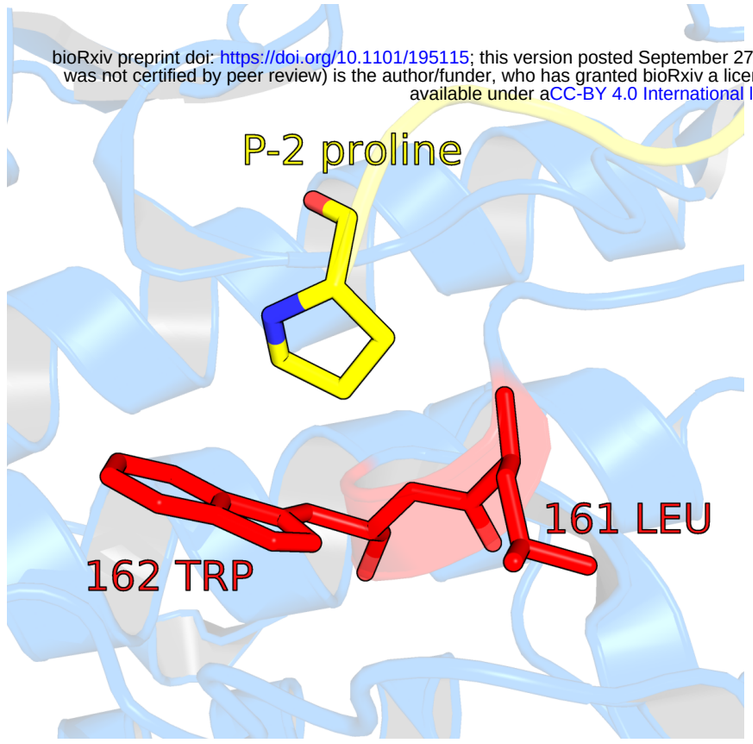

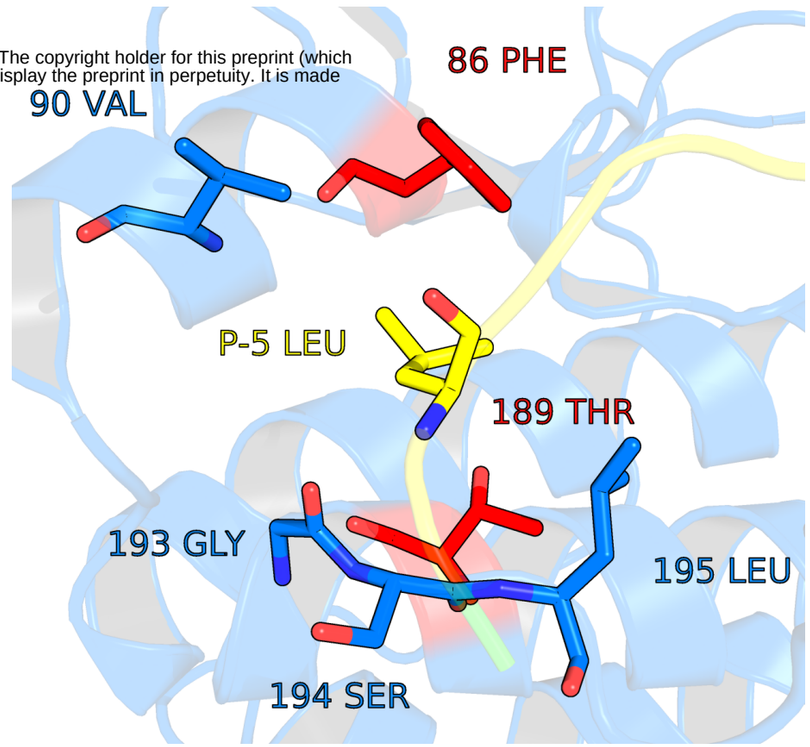

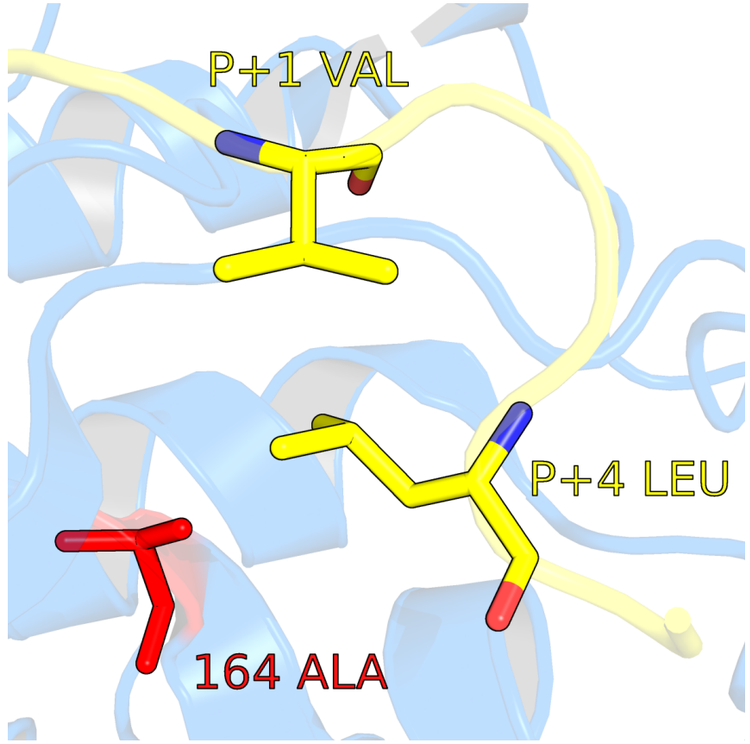

SNF1 kinase

WT, A218L and V244R

incubated with:

WT peptide	VQLKRPA**S**VLALNDL	
Mut D (-5)	VQ**D**KRPA**S**VLALNDL	
Mut A (+4)	VQLKRPA**S**VLA**A**NDL	
	-5 0 +4	

in vitro reaction

mass spectrometry

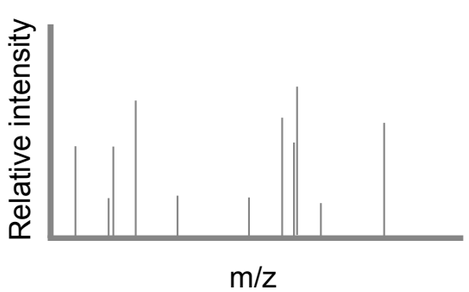

b

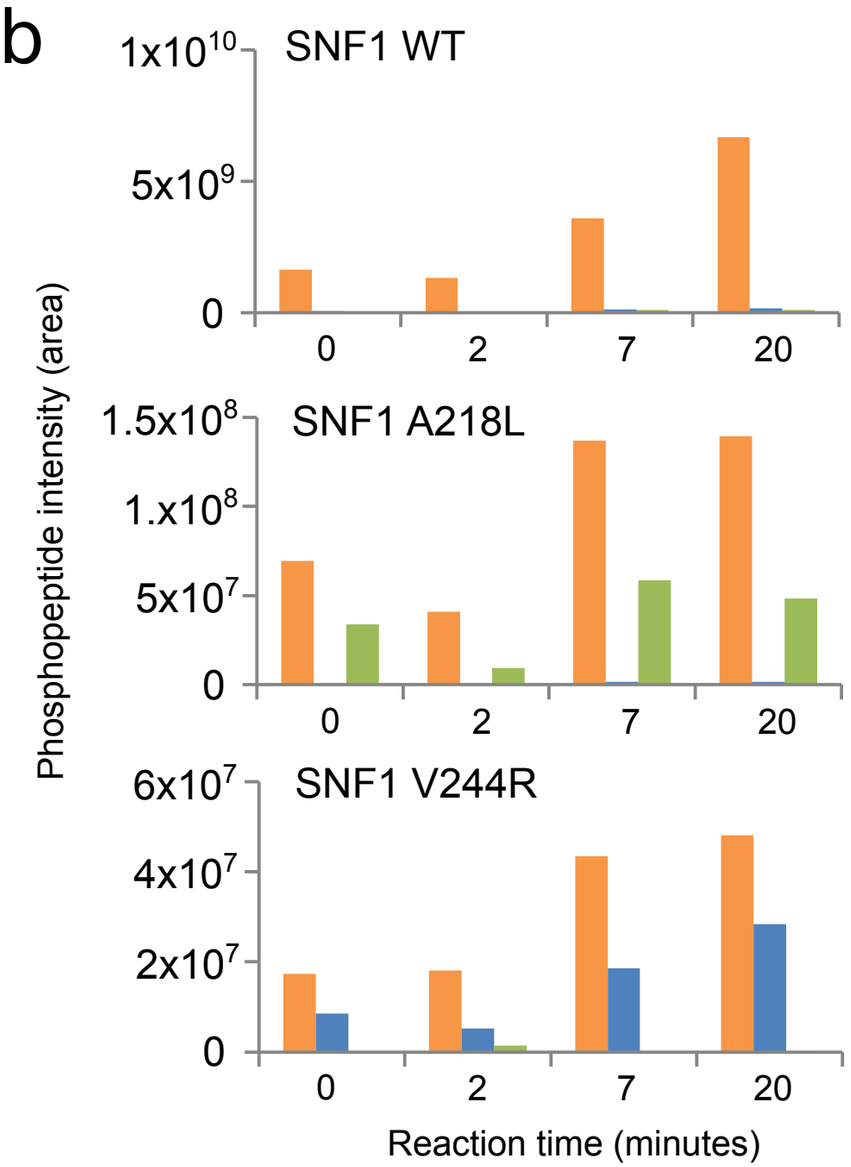

c

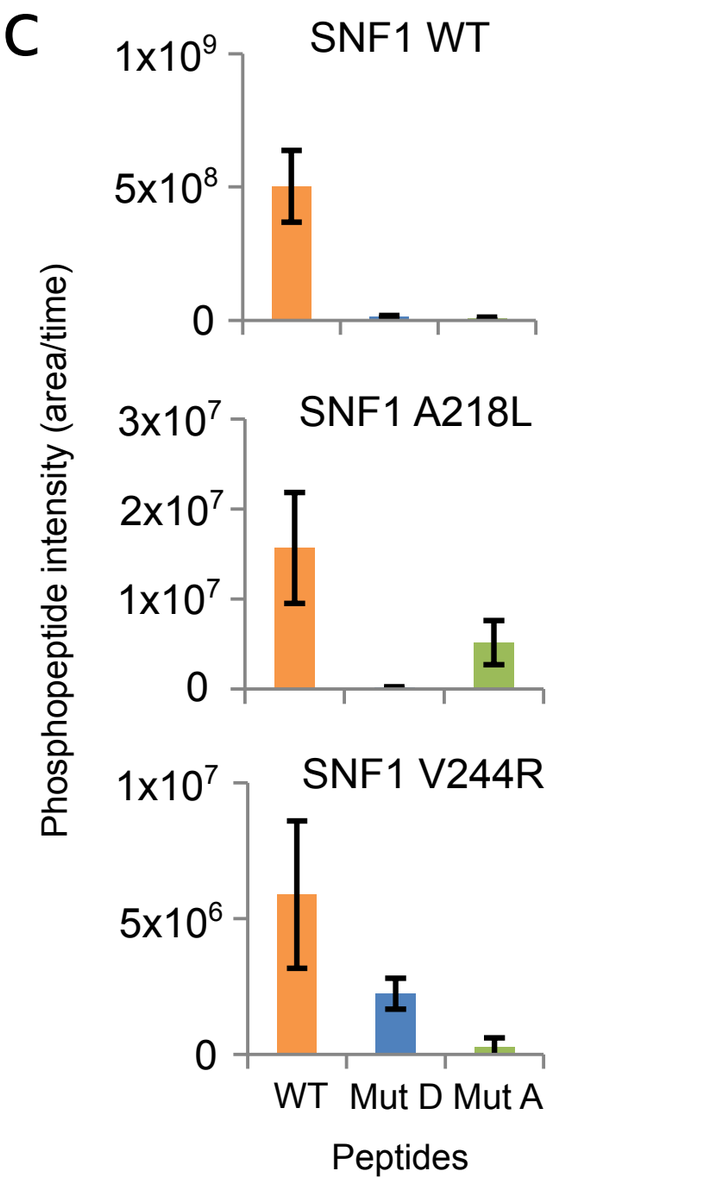

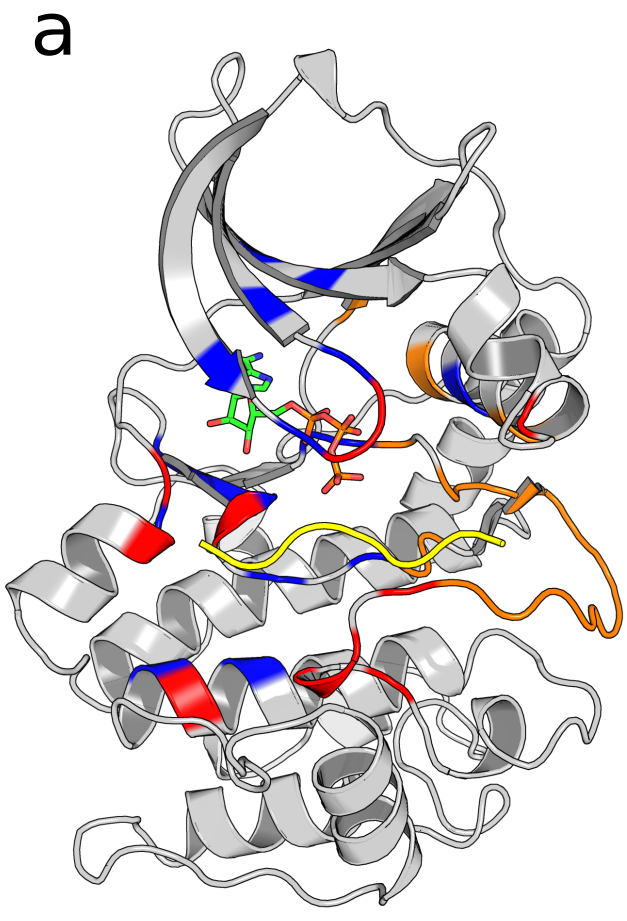
a

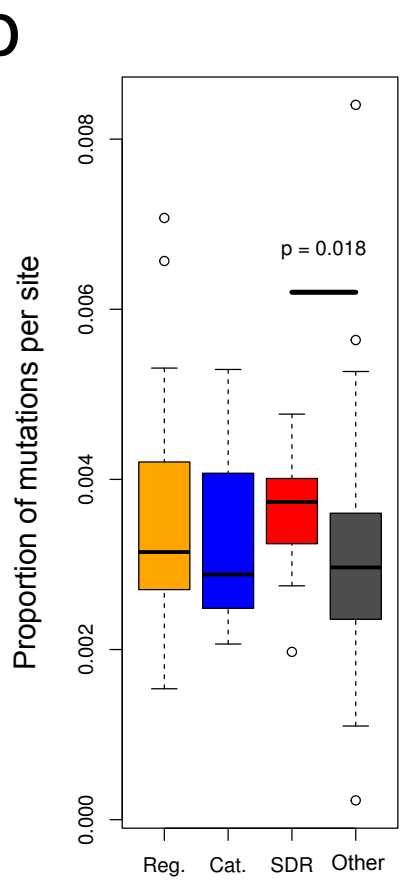
b
Proportion of mutations per site
0.000
0.002
0.004
0.006
0.008
p = 0.018
Reg.
Cat.
SDR
Other

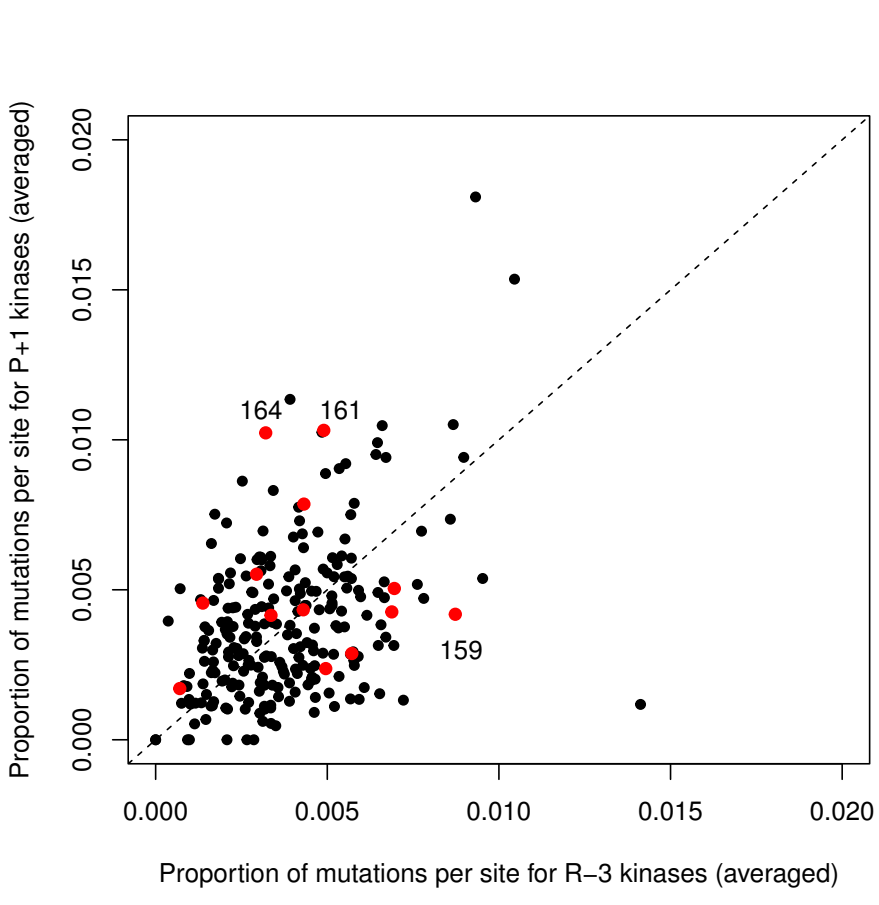
c
Proportion of mutations per site for P+1 kinases (averaged)
0.000
0.005
0.010
0.015
0.020
164
161
159
Proportion of mutations per site for R−3 kinases (averaged)

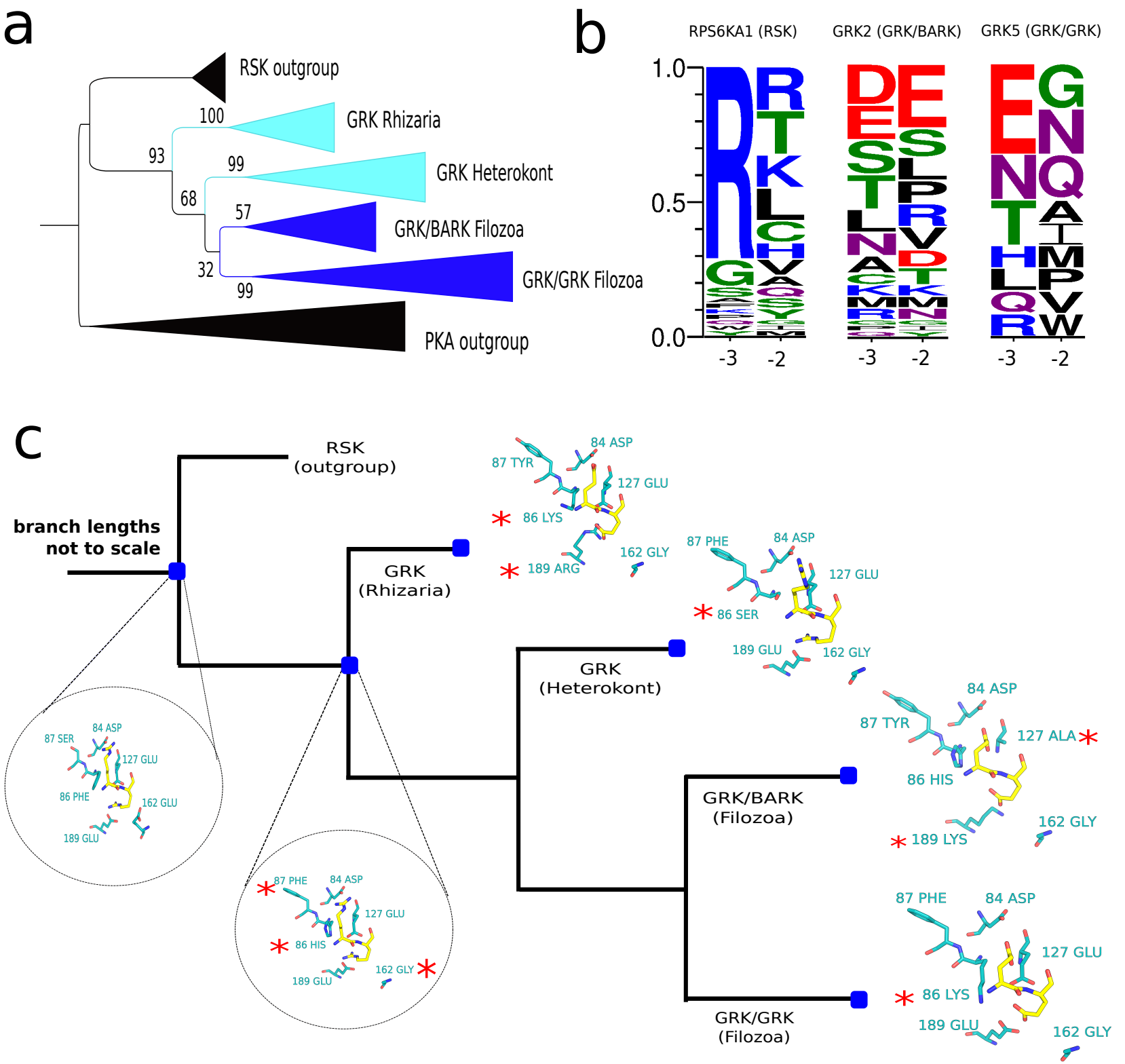
a
RSK outgroup
100
GRK Rhizaria
93
99
GRK Heterokont
68
57
GRK/BARK Filozoa
32
99
GRK/GRK Filozoa
PKA outgroup
b
RPS6KA1 (RSK)
GRK2 (GRK/BARK)
GRK5 (GRK/GRK)
1.0
0.5
0.0
-3
-2
c
RSK
(outgroup)
branch lengths
not to scale
GRK
(Rhizaria)
GRK
(Heterokont)
GRK/BARK
(Filozoa)
GRK/GRK
(Filozoa)
87 SER
84 ASP
127 GLU
86 PHE
162 GLU
189 GLU
87 PHE
84 ASP
127 GLU
86 HIS
189 GLU
162 GLY
87 TYR
84 ASP
127 GLU
86 LYS
189 ARG
162 GLY
87 PHE
84 ASP
127 GLU
86 SER
189 GLU
162 GLY
87 TYR
84 ASP
127 ALA
86 HIS
189 LYS
162 GLY
87 PHE
84 ASP
127 GLU
86 LYS
189 GLU
162 GLY